Aberrant Splicing of a Mouse *disabled* Homolog, *mdab1*, in the *scrambler* Mouse

Marcus L. Ware,*[§] Jeremy W. Fox,*[§]
Jorge L. González,* Nicole M. Davis,*
Catherine Lambert de Rouvroit,[†]
Christopher J. Russo,* Streamson C. Chua, Jr.,[‡]
André M. Goffinet,[†] and Christopher A. Walsh*[‖]
*Division of Neurogenetics
Department of Neurology
Beth Israel Deaconess Medical Center
   and Programs in Neurosciences
   and Biological and Biomedical Sciences
Harvard Medical School
Boston, Massachusetts 02115
[†]Department of Physiology
FUNDP Medical School
61 Rue de Bruxelles
B5000 Namur
Belgium
[‡]Laboratory of Human Behavior and Metabolism
Rockefeller University
New York, New York 10021

Summary

Although accurate long-distance neuronal migration is a cardinal feature of cerebral cortical development, little is known about control of this migration. The *scrambler* (*scm*) mouse shows abnormal cortical lamination that is indistinguishable from *reeler*. Genetic and physical mapping of *scm* identified yeast artificial chromosomes containing an exon of *mdab1*, a homolog of Drosophila *disabled*, which encodes a phosphoprotein that binds nonreceptor tyrosine kinases. *mdab1* transcripts showed abnormal splicing in *scm* homozygotes, with 1.5 kb of intracisternal A particle retrotransposon sequence inserted into the *mdab1* coding region in antisense orientation, producing a mutated and truncated predicted protein. Therefore, *mdab1* is most likely the *scm* gene, thus implicating nonreceptor tyrosine kinases in neuronal migration and lamination in developing cerebral cortex.

Introduction

The cerebral cortex shows a precise layering of multiple neuronal types, with distinct form and function, and this laminar organization is required for normal cognitive function. The cortical neurons are formed in systematic fashion from deepest to most superficial ("inside-out") in specialized proliferative regions deep in the brain. Each newly generated cohort of neurons must migrate as many as thousands of cell body lengths to reach the cortex, and must migrate past previously formed

[§]These authors contributed equally to this work.
[‖]To whom correspondence should be addressed at Division of Neurogenetics, Beth Israel Deaconess Medical Center/Harvard Medical School, Harvard Institutes of Medicine, 77 Avenue Louis Pasteur, Boston, Massachusetts 02115.

neurons to reach their proper cortical layer. Therefore, complex signaling mechanisms must exist to guide and steer migrating cortical neurons, yet virtually nothing is known about the molecular basis of this specialized, targeted neuronal migration. The analysis of mutations that disrupt normal neuronal migration represents a clear avenue to identify genes involved in this process.

The *reeler* mouse was identified several decades ago (Falconer, 1951) and shows severe abnormalities in the patterns of cortical neuronal migration (Caviness, 1982; Goffinet, 1984), as well as having additional defects in cerebellar development and neuronal positioning in other brain regions (Goffinet, 1992). The *reeler* gene has been extensively mapped (Beckers et al., 1994; Bar et al., 1995) and recently cloned (D'Arcangelo et al., 1995; Hirotsune et al., 1995). The gene encodes a large secreted polypeptide, termed Reelin, with a molecular weight of 388 kDa (D'Arcangelo et al., 1995, 1997). Reelin presumably signals through a specific receptor system, although no components of that system have yet been identified.

More recently, an additional mouse mutation, named *scrambler* (*scm*), has been identified with a phenotype very similar to *reeler* (Sweet et al., 1996). *scm* mice show disorganized cerebral cortical lamination (Figure 1A) and cerebellar hypoplasia (Figure 1B). Cerebral cortical neurons show the same dispersion and rough inversion of cortical birth dates that characterize the *reeler* mouse (Gonzalez et al., unpublished data), and detailed analysis of the cerebellar phenotype suggests close similarities to *reeler* (Goldowitz et al., 1997). Furthermore, Reelin protein expression is normal in *scm* mutants in its location and its timing (Goldowitz et al., 1997; Gonzalez et al., unpublished data), suggesting that the *scm* gene may act downstream of the Reelin protein.

In this report, we have genetically mapped the *scm* gene, and identified yeast artificial chromosome (YAC) clones in that region. Sequencing of the YACs identified a gene, *mouse disabled 1* (*mdab1*), as a candidate gene for *scm*. Further analysis showed that the predominant *mdab1* mRNA is abnormal in *scm* mutants, being spliced to a portion of an intracisternal A particle (IAP) retrotransposon element, thus showing that *mdab1* is most likely the causative gene for *scm*.

Results

Genetic Mapping of the *scm* Locus

Since *scm* had been mapped only to a very broad region of chromosome 4 (Sweet et al., 1996), we established a cross to provide further genetic mapping information. The *scm* mutation originally arose in an inbred DC/Le strain that carried the *Dancer* (*Dc*) mutation. The DC/Le strain in turn derived from an obese stock outcrossed to a BALB/c × C3H/He hybrid, crossed again to C3H/HeJ, then inbred (The Mouse Genome Database, 1997). The *scm* mutation was separated from *Dc* by outcrossing a male (+/*Dc*, +/*scm*) to a C3HeB/FeJ female, and intercrossing the normal F1 progeny, and recovering the
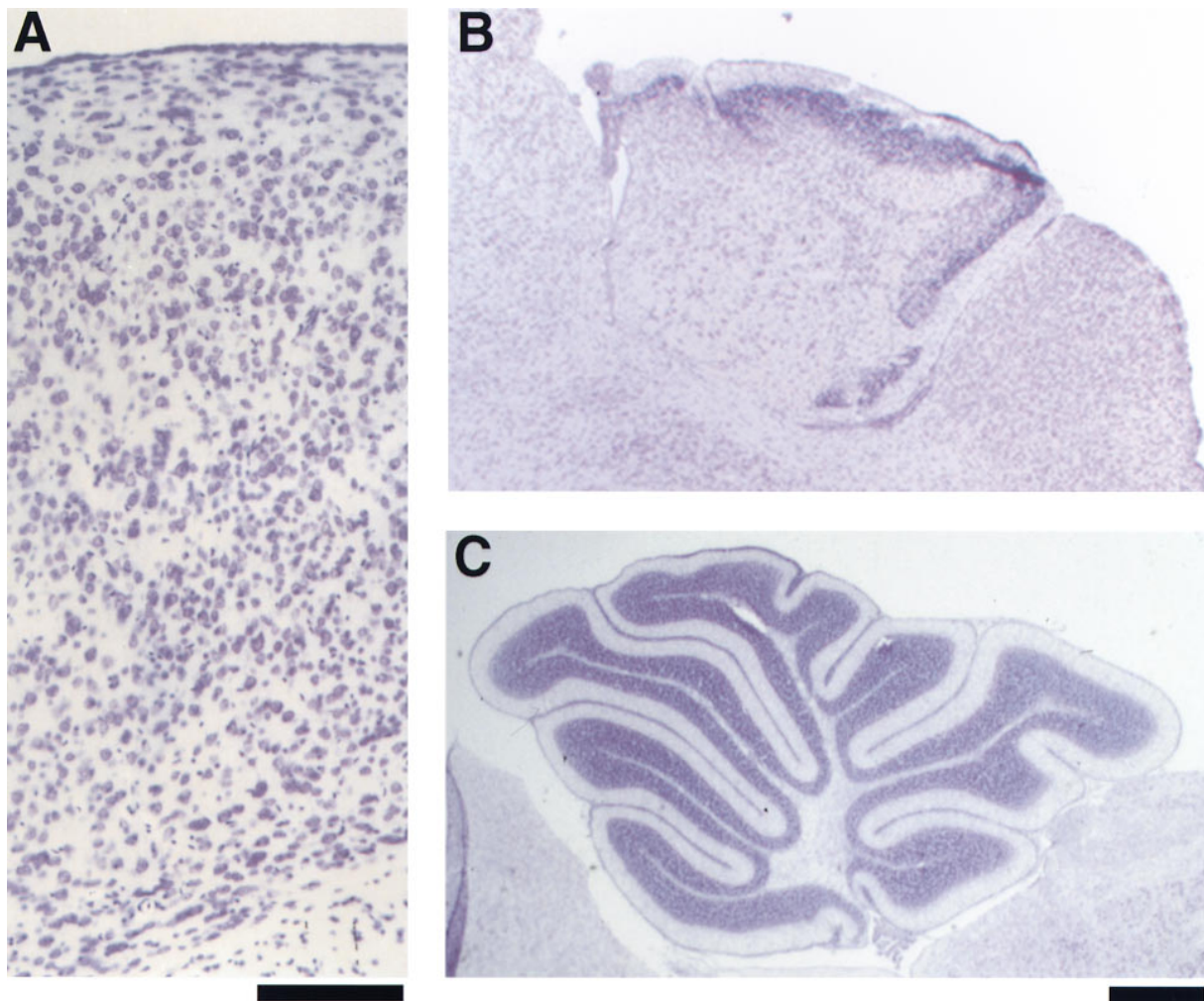
Figure 1. Summary of the *scm* Mutant Phenotype

(A) A parasagittal section of *scm* cerebral cortex. The *scm* cortex shows no clear lamination of cortical neurons, with larger pyramidal neurons scattered at all levels through the cortex. The cortical anomaly will be described in more detail elsewhere (Gonzalez et al., unpublished data). The scale bar shows 200 μm.

(B) A parasagittal section of the *scm* cerebellum. The cerebellum shows severe hypoplasia, with absence of the normal folia and layers. The cerebellar phenotype is described elsewhere (Goldowitz et al., 1997). The scale bar shows 400 μm.

(C) A parasagittal section of the normal cerebellum, for comparison to (B).

scm phenotype in the F2 progeny. The colony at Jackson laboratory was derived from continued inbreeding from that single outcross (Sweet et al., 1996). Therefore, *scm* is originally derived from a strain with a substantial contribution of C3H stock, and has been maintained on a somewhat inbred, albeit mixed strain in which alleles of all tested polymorphic markers match those of the C3H inbred strain. In order to map *scm*, we crossed *scm/scm* homozygotes with $^{+/+}$ C57BL/6 males, and intercrossed the F1 offspring. Homozygous affected offspring of this cross were analyzed with polymorphic microsatellite markers (Ausubel et al., 1994). Heterozygous and wild-type (wt) offspring whose genotype at the *scm* locus could be determined by subsequent crosses were analyzed as well.

Microsatellite marker analysis considerably refined the location of the *scm* gene on chromosome 4. Three *scm/scm* mice were heterozygous for D4Mit31 and additional telomeric markers (Figure 2), suggesting that

D4Mit31 was the closest recombinant marker telomeric to *scm*. One *scm/scm* mouse was heterozygous for D4Mit331 and additional centromeric markers; another *scm/+* mouse showed an independent recombination event between D4Mit331 and *scm*, suggesting D4Mit331 as the closest recombinant marker centromeric to *scm*. These mice, and all other mice analyzed, showed no recombination events between *scm* and D4Mit29, suggesting that D4Mit29 was very close to the *scm* locus and located in between D4Mit331 and D4Mit31 (Figure 2). In a previous mapping cross (Sweet et al., 1996), *scm* showed no recombinants with D4Mit176 in 118 meioses, whereas in our cross, there were two recombinant events with D4Mit176 in 242 informative meioses; however, the map position of *scm* is quite consistent with data from the previous cross (see below).

D4Mit331, D4Mit29, and D4Mit31 have indistinguishable map locations based on the MIT/Whitehead F2 cross originally used to map them (Dietrich et al., 1994,

Markers   **Genotypes**

D4Mit145

D4Mit15

D4Mit175

D4Mit219

D4Mit331

scm

D4Mit29

D4Mit31

D4Mit199

D4Mit334

D4Mit12

| # of animals | 1 | 1 | 1 | 3 | 1 | 1 | 57 | 46 | 9 | 1 |

homozygous Dc/C3H   heterozygous   homozygous C57BL/6   not tested
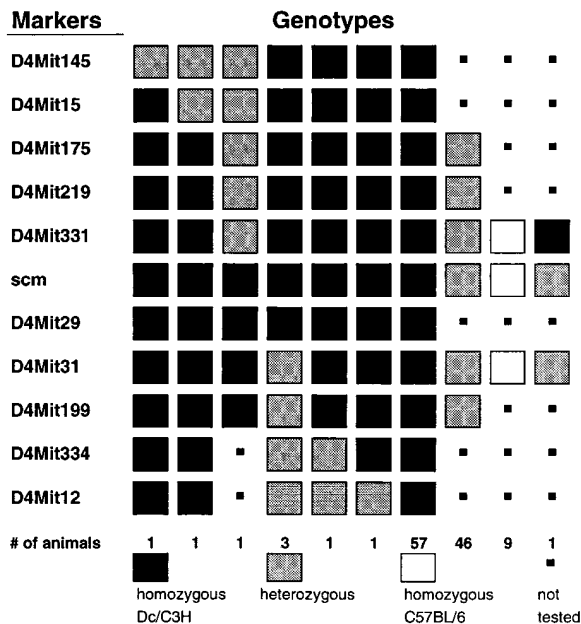
Figure 2. Genetic Mapping of the *scm* Gene Based on 242 Informative Meioses

Genotypes summarize the results of intercrossing the progeny of *scm/scm* mice on a mixed C3H and Dc/LE background crossed to $^{+/+}$ *C57BL/6* mice. D4Mit176 is flanked by D4Mit175 and 219; since 175 showed a large size difference by PCR, 175 was routinely analyzed instead.

1996), and could not be ordered using existing physical maps because the markers are not all included on any published YAC contigs (Copeland et al., 1993; Whitehead Institute/MIT Center for Genome Research, 1996). Therefore, we analyzed a large number of mice from a previous cross (Chua et al., 1996) used to map the diabetic (*db*) gene, since *db* and *scm* map very close to one another (Figure 3A). The mice that were analyzed were obese progeny from a cross between C57BL/KsJ-$m^{+/+}db$ and MA/MyJ mice (Chua et al., 1996). This particular cross was chosen because the parental strains were informative for most of the known markers in the region near *db* and *scm*. All 492 mice from that cross were typed for the markers D4Mit176 and D4Mit31. Mice showing recombinant chromosomes were subsequently typed for the intervening markers, D4Mit167, 219, 29, 46, 75, 306, and 168. This generated a map showing that D4Mit331 was located 0.6 cM proximal to D4Mit29/*scm*, while D4Mit31 was located 0.8 cM distal. *scm* was located ≈1.2 cM from D4Mit176, consistent with the published map location presented previously (Sweet et al., 1996), which had suggested a 95% confidence interval for the location of *scm* that was <2 cM from D4Mit176. The genetic map of the *scm* region formed a framework for physical mapping.

Physical Mapping of the *scm* Locus

Several YACs have been previously identified that contain markers D4Mit167, 118, 219, 331, 75, and D4Mit31 (Copeland et al., 1993; Chua et al., 1996; Whitehead Institute/MIT Center for Genome Research, 1996), and we confirmed the marker content of these YACs (Figure 3B). Since no YACs have been identified as containing

D4Mit29 and D4Mit46, the markers closest to *scm* genetically, we screened the MIT/Whitehead Institute YAC library to identify YACs containing D4Mit29. Three YACs were identified (Figure 3B): 62D7, 37G4, and 175A2. Pulse field gel analysis indicated that 62D7 was 300–500 kbp, 37G4 was 500–800 kbp, and 175A2 was 1220–1500 kbp. As expected, these YACs were novel with no previous hits in known physical maps of the mouse genome (Whitehead Institute/MIT Center for Genome Research, 1996). Analysis of marker content in each of the YACs indicated that they still did not form a continuous contig across the *scm* region. Therefore, we began DNA sequence analysis of these YACs for the purposes of closing the contig.

Identification of *mdab1* as a Candidate Gene for *scm*

In order to generate additional STSs to close the YAC contig around the *scm* locus, interspersed repetitive sequence PCR (IRS–PCR) was performed (Hunter et al., 1994) on a pooled preparation of the three YACs that contained D4Mit29, the most closely linked marker to the *scm* locus. IRS–PCR is a method that allows rapid generation of YAC contigs (Hunter et al., 1996) by amplification of nonrepetitive DNA located adjacent to IRS, using primers homologous to the repetitive sequences. IRS–PCR was performed with primer B1MvsCh (Hunter et al., 1994). IRS–PCR products were pooled, cloned, and sequenced. One IRS–PCR product (Figure 3C) contained a DNA fragment, presumably representing a single exon, that showed 100% identity at the nucleotide level over 60 bp to the *mdab1* gene (Howell et al., 1997). *mdab1* was previously identified in a two hybrid screen by virtue of the binding of its protein product to Src. The protein is intensely expressed in developing neurons throughout the nervous system, and is concentrated in growing neurites (Howell et al., 1997). The Drosophila homolog, *disabled*, is essential for normal neuronal development and process outgrowth (Gertler et al., 1993). Therefore, we tested *mdab1* as a candidate gene for *scm*. Our interest in *mdab1* as a candidate gene for *scm* was strengthened by the public presentation of the *mdab1* knockout phenotype (Howell, B. W., Hawkes, R., Soriano, P., and Cooper, J. A., unpublished data).

Northern analysis, using polyA-selected RNA from normal fetal mouse embryo, showed the same pattern of three alternative *mdab1* transcripts described previously (Howell et al., 1997), when probed with a PCR product corresponding to the 5′ end common to the three characterized transcripts (Figure 4A). The 5′ probe showed hybridization to bands of 5, 3.1, and 1.3 kb (Howell et al., 1997). In Northern blots prepared from polyA-selected RNA from neonatal and adult mouse brains, the same 5, 3.1, and 1.3 kb bands were present (Figure 4B); in similar Northern blots performed using total RNA from adult and neonatal brains (data not shown), the 5 kb transcript was the only band that was clearly seen, so the 5 kb transcript appears to represent the predominant *mdab1* splice form in brain.

At least three *mdab1* cDNAs have been cloned, and have been named based on the number of amino acids in the predicted protein product: 555, 271, and 217 (Howell et al., 1997) (see Figure 5A). cDNA 555 encodes a
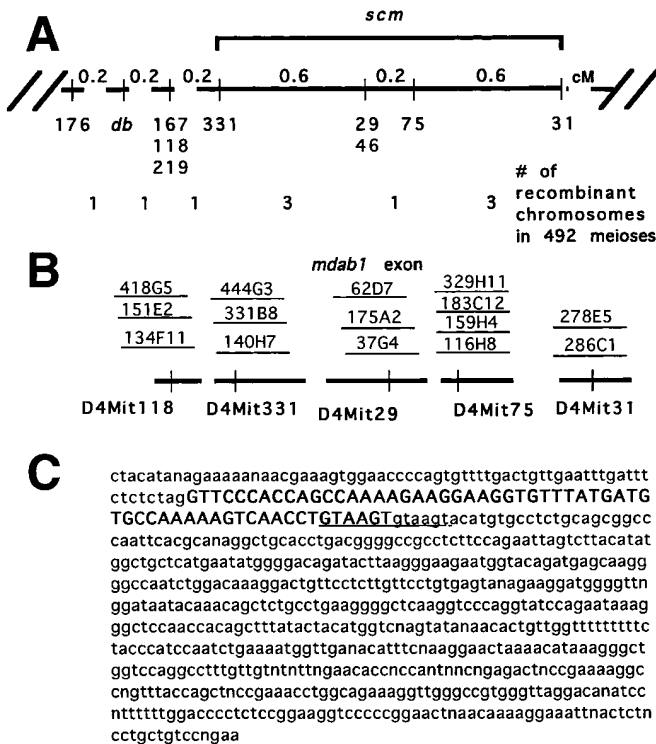
A

scm

```
      0.2   0.2   0.2    0.6      0.2      0.6
//─+──+──+──+───────────+─────────+─────────────+──cM //
   176  db  167  331         29   75              31
            118                                   
            219          46                       
                                              # of
    1    1    1    3         1          3     recombinant
                                              chromosomes
                                              in 492 meioses
```

B

mdab1 exon

```
418G5     444G3     62D7     329H11
151E2     331B8     175A2    183C12          278E5
134F11    140H7     37G4     159H4           286C1
                             116H8
   ──────    ──────   ──────   ──────        ──────
    ┼         ┼         ┼        ┼             ┼
D4Mit118  D4Mit331  D4Mit29  D4Mit75      D4Mit31
```

C

```
ctacatanagaaaaanaacgaaagtggaaccccagtgttttgactgttgaatttgattt
ctctctagGTTCCCACCAGCCAAAAGAAGGAAGGTGTTTATGATG
TGCCAAAAAGTCAACCTGTAAGTgtaagtacatgtgcctctgcagcggcc
caattcacgcanaggctgcacctgacggggccgcctcttccagaattagtcttacatat
ggctgctcatgaatatggggacagatacttaagggaagaatggtacagatgagcaagg
ggccaatctggacaaaggactgttcctcttgttcctgtgagtanagaaggatggggttn
ggataatacaaacagctctgcctgaaggggctcaaggtcccaggtatccagaataaag
ggctccaaccacagctttatactacatggtcnagtatanaacactgttggttttttttc
tacccatccaatctgaaaatggttganacatttcnaaggaactaaaacataaagggct
ggtccaggcctttgttgtntnttngaacaccnccantnncngagactnccgaaaaggc
cngtttaccagctnccgaaacctggcagaaaggttgggccgtgggttaggacanatcc
ntttttggacccctctccggaaggtcccccggaactnaacaaaaggaaattnactctn
cctgctgtccngaa
```

predicted protein of 555 amino acids, with an apparent molecular weight of 80 kDa (Howell et al., 1997). cDNA 271 differs from 555 in having an exon of 270 nucleotides, which encodes a stop codon, inserted at nt position 986 of the 555 sequence (Howell et al., 1997). The same Northern blots analyzed with a probe corresponding to the 3′ end common to the 555 and 271 cDNAs showed hybridization to all three bands (5, 3.1, and 1.3 kb). A third cDNA, 217, diverges at nucleotide 860. However, Northern analysis with a probe corresponding to the 3′ end of the 217 cDNA did not show hybridization to any of the three bands (not shown), suggesting that the 217 cDNA is not expressed in the mouse embryo or perinatal brain at levels detectable by Northern blot. A
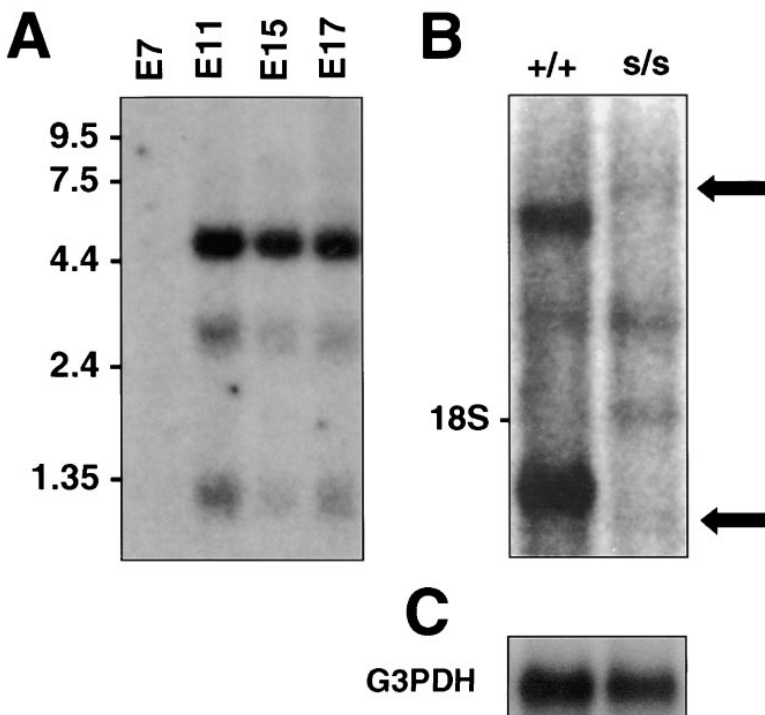

Figure 4. Northern Analysis of mdab1 in Normal and scm Mutant Mice

(A) A Northern blot of fetal mouse RNA (polyA-selected) from E7, E11, E15, and E17 animals. Size standards are indicated. The blot was hybridized with a PCR-generated probe (using primers C and E, Table 1) that corresponds to the 5′ end common to all illustrated transcripts, and shows hybridization to bands of 5, 3.1, and 1.3 kb.

(B) A Northern blot from wt and scm/scm animals (age P12–14 and adult, respectively) hybridized with the same probe used in (A). The normal mouse brain RNA shows three bands that are indistinguishable from those present in the mouse embryo blots in (B). A faint fourth band (18S) represents cross-hybridization of the probe to a small amount of 18S ribosomal RNA that remained after polyA-selection. In scm/scm homozygotes, the 5 kb message is faint and ≈1500 bp larger than normal (arrow); the 3.1 kb message is not obviously changed, and the 1.3 kb message appears to be decreased both in size (by 100–200 bp) and intensity (arrow).

(C) The blot shown in (B) after hybridization to a G3PDH probe to control for loading of RNA.
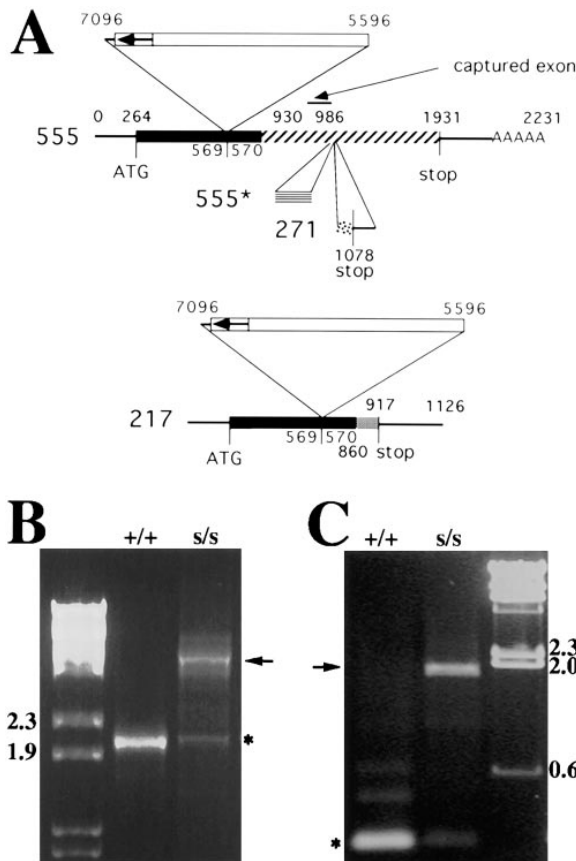
Figure 5. RT–PCR Products from the Coding Region of *mdab1*

(A) All known cloned cDNAs of *mdab1*, based on (Howell et al., 1997) and RT–PCR data. cDNA 555 encodes a protein of 555 amino acids, with an apparent molecular weight of 80 kDa. cDNA 271 differs from 555 in having an exon of 270 nucleotides inserted at nucleotide position 986. The inserted sequence encodes a stop codon, producing a sequence predicted to encode only 271 amino acids. cDNA 217 shares a common 5′ end with 271 and 555, but diverges at nt 860, encoding a protein predicted to contain 217 amino acids. A fourth, partially characterized cDNA (555*) corresponds at least in part to 555, but contains an additional exon inserted at position 980; its 3′ end is not known. All three characterized cDNAs—555, 271, and 217—show an insertion of 1.5 kbp of sequence between nt 569–570 in *scm* mice (see below).

(B) "Long" RT–PCR products using primers complementary to bp 1–25 and 2050–2074 of the cDNA sequence of the 555 transcript (primers A and O, Table 1). In wt animals, the band of expected size was produced, and the identity of this band was confirmed by nested PCR reactions using this product as template. *scm/scm* mutants show a little PCR product at the expected size (asterisk), with a prominent higher molecular weight band ≈1.5 kbp larger than normal (arrow). Similar results were obtained with five different primer pairs that occurred near the extremes of the 555 transcript.

(C) RT–PCR products from wt and *scm/scm* mutants from the segment of the cDNA between 491–626, showing the minimal region from which the abnormally large cDNA can be amplified. The RT–PCR product of primers P and E (Table 1) is shown. The PCR product size predicted from the known cDNAs for *mdab1* is 172 bp, and is shown by the strong band at the asterisk. The reaction in *scm* mutants produced a small amount of product of the expected size (asterisk) after 30 cycles of PCR, with a prominent band 1.5 kbp larger than expected (arrow). Two additional fainter larger PCR products in the wt cDNA reaction probably represent specific products; they may correspond to additional alternative splice products that are also abnormal in *scm* mutants. PCR reactions after larger numbers of cycles tended to show relatively more of the normal-

fourth transcript, 555,* only identified as a fragment, contains an additional exon inserted at approximately position 980 of the 555 cDNA (Howell et al., 1997). One or more bands on the Northern blots may correspond to as yet uncharacterized splice products.

The exon identified by IRS–PCR matches bp 927–986 of the published sequence of the 555 and 271 transcripts, and encodes the splice donor site at which these two sequences diverge. Furthermore, the captured exon contains a tandem repeat sequence that appears to encode two serial splice donor sites (GTAAGTGTAAGT) (Shapiro and Senapathy, 1987). The second of the splice donor sites is evidently spliced to two different exons in order to form the 555 and 271 transcripts. In addition, the first of the two splice donor sites is spliced to a third exon, in a different reading frame, forming the 555* fragment (See Figure 5A).

Abnormal Expression of *mdab1* in *scm* Brain

In Northern blots prepared from neonatal or adult brain RNA from *scm/scm* homozygotes, at least two *mdab1* mRNAs migrated at aberrant rates. The predominant, 5 kb message was not detectable at its normal size, but as a presumably corresponding band ~1.5 kb larger than normal (Figure 4B). The 3 kb message did not appear to be obviously changed in size and intensity. The 1.3 kb message was also undetectable at its normal size, with a novel band appearing at 100–200 bases smaller size (Figure 4B). Northern analysis of polyA-selected RNA from *scm/+* heterozygotes showed the expected mixture of abnormal and normal splice products (data not shown). Northern analysis of total RNA from P1 normal and *scm/scm* mice also showed a shift of the 5.0 kb transcript to higher molecular weight in *scm* mutants, although no obvious decrease in its abundance; Northern analysis of total RNA did not visualize the smaller *mdab1* transcripts clearly (data not shown). These data suggest at least two *mdab1* mRNAs of abnormal size in *scm* mutants.

Southern analysis of DNA from *scm/scm* and normal mice was performed using multiple restriction enzymes (BamHI, BglII, EcoRI, KpnI, TaqI, and MspI) and multiple overlapping PCR-generated probes that covered the entire coding region of the 555 transcript. No bands were observed that were polymorphic between *scm* mutant mice and wt C3H or C57BL/6 mice (data not shown), suggesting that the *scm* mutation may produce abnormal splicing of the *mdab1* gene without grossly disrupting its genomic structure.

We confirmed that *scm* mutant mice carry an abnormally large mRNA for the *mdab1* gene by amplifying *mdab1* cDNAs using reverse transcription–polymerase chain reaction (RT–PCR). We used primers designed to match the published sequence of the 555 transcript in "long" RT–PCR in normal and *scm/scm* mutant mice. cDNA prepared from normal C3H or C57BL/6 mice gave

sized band in *scm* mutants, presumably reflecting preferential amplification of the smaller fragment, which appears to be far less abundant. DNA size standards are lambda digested with BstE (B) or HindIII (C), and sizes of some standard fragments are indicated with numbers.

Table 1. Sequences of PCR Primers Used to Amplify *mdab1*, and Regions of Complementarity to the Published Sequences (Howell et al., 1997)

Name	Primer Sequence	Transcript Amplified	Location
A	5′-CCCAGCTCGGCGCTCACCCGGGCTT-3′	555, 271, 217	1–25
B	5′-CCGGGCTGGAGAGCGCGTTTGAGTG-3′	555, 271, 217	28–52
C	5′-AGGGAGGAGCCTTTCTCTTG-3′	555, 271, 217	177–196
D	5′-CCATGATGAAGCTCAAGGGT-3′	555, 271, 217	454–473
E	5′-TGTGATGTCCTTCGCAATGT-3′	555, 271, 217	626–607
F	5′-AAGGATAAGCAGTGTGAACAAG-3′	555, 271, 217	789–810
G	5′-CAGCCAAAAGAAGGAAGGTG-3′	555, 271	935–954
H	5′-TGGGTCACAGCACTTACAGG-3′	555, 271	997–978
I	5′-TCTAGATCTCCCATCACGGC-3′	217	1049–1030
J	5′-CAGCAGTGCCGAAAGACATA-3′	555	1146–1127
		271	1416–1398
K	5′-TTCATGCCCACACAAACTGT-3′	555	1359–1378
		271	1629–1648
L	5′-ACTTCAACAAAGTCGGGGTG-3′	555	1600–1619
		271	1870–1888
M	5′-TGGAGAAGGCCTCTGAGGTA-3′	555	1596–1577
		271	1866–1847
N	5′-GGGATGCTGATGATTTGGAT-3′	555	1758–1739
		271	2028–2009
O	5′-GTGAGGTGAGAGCCCAAGAG-3′	555	2074–2055
		271	2344–2325
P	5′-TTCCAAGGGAGAACACAAACAG-3′	555	491–513

a band of ≈2 kbp, the predicted size (Figure 5B). In contrast, cDNA from *scm* mutant mice produced only slight amplification of the normal-sized band, and showed a prominent band ≈1.5 kbp larger (Figure 5B). Although the 217 transcript was not detectable by Northern blot, primers specific for the 217 transcript amplified RT–PCR products of predicted size from total brain RNA, and amplified an additional band from *scm* mutants ≈1.5 kbp larger than the PCR product from normal mice. Thus, *scm* mutants carry alterations affecting multiple alternative transcripts of the *mdab1* gene. The fact that both the 555 and 217 transcripts are abnormal suggests that the abnormality affects the 5′ end of the *mdab1* message (nt 0–860). The shorter size of the 1.3 kb band on Northern blot probably reflects abnormal splicing of yet another *mdab1* splice product not yet characterized fully.

In order to map the specific region of the *mdab1* gene that is spliced abnormally, shorter PCR reactions from segments of the 555 and 217 transcripts were performed. Any PCR reaction that amplified nt 491–626 of the 555 cDNA (Table 1, primers E, P) produced an additional band, 1.5 kbp larger than the expected product (Figures 5B and 5C). PCR products from most of the conserved 5′ end common to both transcripts (nt 0–454) were normal; PCR products from the 3′ end of the 555 transcript were also normal (nt 935–2074). These data strongly suggest that the sequence inserted into the cDNA is located between bp 491 and 626 of the 555 sequence, and affects all known *mdab1* cDNAs. Although in these PCR reactions a significant band at normal size was seen in *scm/scm* homozygotes, Northern analysis suggests that the normal transcripts are essentially undetectable (Figure 4B). Normal transcripts are likely rare in *scm/scm* homozygotes, but preferentially amplified by PCR because they are so much shorter (1.5 kbp) than the corresponding mutant products.

Insertion of IAP Retrotransposon Sequences into the *mdab1* mRNA in *scm* Mice

DNA sequence analysis of the abnormally large PCR products showed that the bulk of the sequence inserted into the cDNA matched sequences of IAP elements (Lueders and Kuff, 1987; Kuff and Lueders, 1988), suggesting that IAP sequences are inserted into the coding region of the *mdab1* gene in antisense orientation. The DNA sequence of the *scm*-specific, abnormally large bands matched the wt sequence through nt 569 (Figure 6), after which it abruptly changed. For a 28 bp sequence, the DNA sequence showed no clear identity to sequences in the GenBank databases; thereafter, beginning with the sequence TGTTA, the sequence matched the 3′ long terminal repeat (LTR) of many IAP elements (beginning at nt 7091 of the published IAP sequence, and proceeding 3′ to 5′ from there). The match to IAP sequences continued for ~1.5 kbp, after which the sequence abruptly switched to being a perfect match to the bona fide 555 transcript of *mdab1* beginning at nt 570.

In order to determine whether the IAP sequences were inserted within an exon or joined to the cDNA via splicing events, we used vectorette PCR to determine genomic DNA sequences at the splice junctions in *scm* mutants and mice of the DC/Le parental strain. No IAP sequences were found within 2kbp of either exon boundary, demonstrating that the IAP sequence is inserted into the cDNA sequence via splicing. In *scm* mutants the normal 5′ splice donor sequence and the normal 3′ splice acceptor sequence matched the sequences in DC/Le DNA at the most highly conserved positions at the intron boundaries (Figure 7), as well as in the 3′ acceptor region necessary for branch formation. Sequences of the cryptic splice donor and acceptor sequences in *scm* (Figure 7) closely matched splice consensus sequences (Shapiro and Senpathy, 1987), and did not differ between *scm* and DC/Le mice at any of the most highly conserved

mdab1 coding sequence

aa92	S	F	G	G	I	K	I	F	D	E	K	T	G

nt531 TCCTTTGGAGGAATCAAAATCTTTGATGAGAAGACGGGG

IAP 3' LTR

ATCCCCCCTGGGATAATGGGGTAAGGACTGTTATTCGACGCG

TTCTCACGACCGGCCAGGAAGAACACCACACACCAGAATCTT

CTGCGACAAAGCTTTATTCTTACATCTTCAGGAAAAGAG

-------- 1200 bp --------

IAP sequence

ACCTGTCCAGACAGAGCCAAGGCTGTGTGAATTAAGGCCAAA

CCCAGTTCGTAGTTAGTGGTAAAAAAGCAGGAGAATACTTGA

GCATTATACATCACCGTCATTGGGAGTGGAAATGTGGACATT

ATCCCCAACGCTGCTCTCTCTTTATTAGTGACGCCCTGGAC

ATCACCAAGACGAGGGACATTAGTATTCCCTTGGTCAGTCTG

mdab1 coding sequence

GATTTTCGGGCCCTTCAGCATCACCATGCTGTT

Figure 6. DNA Sequence of the Abnormally Large cDNA Found in *scm* Homozygotes

The illustrated sequence begins at nt 531 of the *mdab1* cDNA (encoding aa 92), shown by the solid line above the sequence. After nt 569, the sequence deviates completely from the normal cDNA sequence. After 28 nucleotides, the abnormal sequence matches that of an IAP element 3' LTR in antisense orientation, shown by the interrupted line above the sequence. Sequence match to the IAP sequence continues for 1.5 kbp, after which the sequence is again identical to the *mdab1* coding sequence beginning at nt 570.

splice site residues (Shapiro and Senpathy, 1987). Some polymorphisms were uncovered, however, at sites not predicted to influence splicing events. Additionally, *scm* mice appear to have a 200–300 bp deletion within the IAP several hundred bases downstream of the cryptic donor sequence (data not shown). It is likely that an apparently benign base substitution, or the small IAP deletion, is responsible for the preferential utilization of the cryptic splice sites in *scm* mutants.

IAP elements are increasingly commonly recognized as causing insertional mutations in mice (Amariglio and Rechavi, 1993). They occur in ~1000 copies per haploid genome (Lueders and Kuff, 1987; Kuff and Lueders, 1988) and appear to cause mutations by a variety of mechanisms. Some agouti mutations result from IAP insertions that activate transcription (Michaud et al., 1994), or cause ubiquitous expression by virtue of the LTR promoter elements in the IAP (Duhl et al., 1994). Other IAP insertions appear to affect levels of transcription by mechanisms that are not as clear (Hamilton et al., 1997). Recently, the Albany allele of *reeler* has been shown to be caused by an IAP insertion within an exon that causes skipping of that exon (Royaux et al., 1997).

The predicted consequences of inserting intronic and IAP element sequences in antisense orientation into the coding region of *mdab1* are substantial. Amino acids 8–196 of mDab1 form the phosphotyrosine binding (PTB) domain, which is required for interaction with nonreceptor tyrosine kinases, and which shows substantial sequence conservation with other PTBs (Howell et al., 1997). The inserted sequences completely change the predicted amino acid sequence of the protein beginning at amino acid 103, in the middle of the PTB. The IAP 3' LTR encodes multiple stop codons in all reading frames, so that the protein is predicted to be severely truncated as well. Furthermore, the mutation affects all known cloned cDNAs of *mdab1*.

Discussion

In this report, we have mapped the *scm* locus by using two distinct mouse crosses. We have identified YACs from this region, and shown that three YACs contain a fragment of the *mdab1* gene. Northern analysis showed that *scm* mice produce abnormal *mdab1* RNAs, such that the most abundant transcript is not present at its normal size. The abnormal RNA contains a segment of intronic sequence and 1.5 kbp of IAP element sequence inserted in an antisense orientation; finally, we determined that the insertion occurs by aberrant splicing of the *mdab1* gene.

Since mDab1 was identified by virtue of its physical binding to Src, the identification of *mdab1* as the *scm* gene likely implicates nonreceptor tyrosine kinases such as Abl, Src, and Fyn in the control of neuronal migration. Assuming that mDab1 exerts its essential role by interacting with nonreceptor tyrosine kinases (for which there is as yet no direct evidence), it is not clear which kinases are actually utilized. Although Fyn appears to mediate neural cell adhesion molecule–dependent neurite outgrowth (Beggs et al., 1994) and constitutively associates with neural cell adhesion molecule 140 (Beggs et al., 1997), engineered mutations in *fyn* (Stein et al., 1992) cause an excess of hippocampal pyramidal cells and dentate gyrus granule cells, but no clear reported defect in neuronal migration (Grant et al., 1992). Similarly, Src is necessary for L1CAM-mediated axon outgrowth (Ignelzi et al., 1994), and Src appears to be necessary for neurite outgrowth in response to calcium influx, by activating a downstream cascade including Ras and MAP kinase (Rusanescu et al., 1995); however, mutations in *src* (Rusanescu et al., 1995) or *abl* (Schwartzberg et al., 1991; Tybulewicz et al., 1991) have not been reported to cause abnormalities in neuronal migration. Mice mutant for both *src* and *fyn* die neonatally, but do not appear to have a specific disorder in neuronal
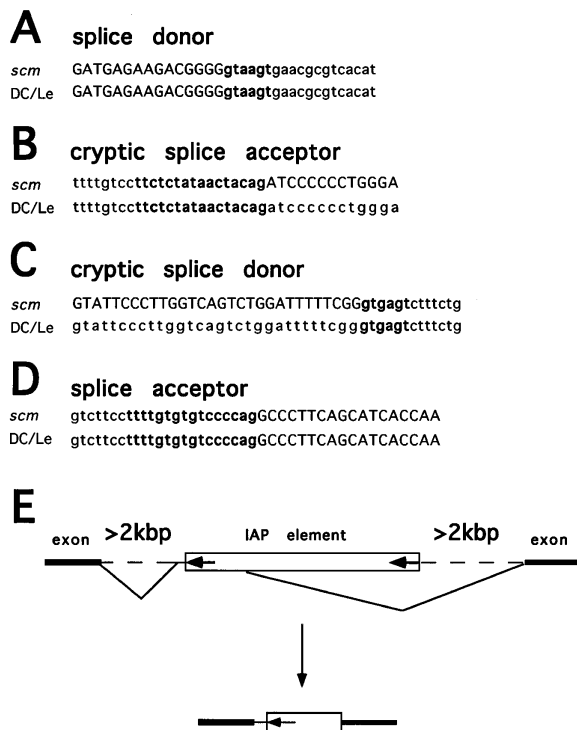
A splice donor

scm   GATGAGAAGACGGGGgtaagtgaacgcgtcacat
DC/Le GATGAGAAGACGGGGgtaagtgaacgcgtcacat

B cryptic splice acceptor

scm   ttttgtccttctctataactacagATCCCCCCTGGGA
DC/Le ttttgtccttctctataactacagatccccccctggga

C cryptic splice donor

scm   GTATTCCCTTGGTCAGTCTGGATTTTTCGGgtgagtctttctg
DC/Le gtattcccttggtcagtctggattttttcgggtgagtctttctg

D splice acceptor

scm   gtcttccttttgtgtgtccccagGCCCTTCAGCATCACCAA
DC/Le gtcttccttttgtgtgtccccagGCCCTTCAGCATCACCAA

E

Figure 7. DNA Sequence Analysis of Splice Junctions in Normal DC/Le Mice and *scm* Mutants

A shows the sequence of the 5' splice donor near nt 569 beginning in the coding region (upper case) and extending into the intron (lower case). The intron sequence at the splice junction (bold) conforms well to the consensus (gtaagt) (Shapiro and Senapathy, 1987) and is identical in *scm* and Dc/Le mice. No IAP sequences were found within 2 kbp of the splice junction.

B shows the sequence of the cryptic splice acceptor in the intron of *mdab1*. Once again the sequence is the same in *scm* and DC/Le mice, and forms a close match to a consensus 3' acceptor sequence, with a good (9/12) polypyrimidine stretch and conserved cag sequence at the splice junction.

C shows the sequence of the cryptic splice donor sequence. The sequence is again the same in *scm* and DC/Le mice, and forms a close match to a consensus splice donor sequence.

D shows the sequence of the normal 3' splice acceptor site, which does not contain IAP sequences, and which is again not polymorphic between *scm* and Dc/Le near the splice site. Polymorphisms between *scm* and DC/Le mice are not uncommon at other sites within the cryptic exon however, including base substitutions and a 200–300 bp deletion; one or more of these other polymorphisms presumably cause utilization of the cryptic splice sites.

migration (Stein et al., 1994). However, mutations in *csk*, which encodes a negative regulator of Src, cause a severe CNS phenotype (Imamoto and Soriano, 1993) that seems to rely on Src and Fyn (Thomas et al., 1995). Hence, the functional redundancy of members of the Src family of tyrosine kinases may make genetic dissection of their functions difficult.

Although mDab1 was identified based on its physical binding to Src (Howell et al., 1997), it is homologous to Drosophila *disabled*, which has been implicated in neuronal development through genetic interactions with the Drosophila *abl* (*Dabl*) gene (Gertler et al., 1993). Another gene identified based on its interaction with *Dabl*, *enabled*, has a mouse homolog, MENA, that has recently

been critically implicated in migration of non-neuronal cells (Gertler et al., 1996). Other genes that interact with *Dabl* included *fax* and *prospero* (Gertler et al., 1993), and these mutants caused abnormalities of neuronal process outgrowth as well. Kinases such as Src have been implicated for some time in axon outgrowth (Cox and Maness, 1992). Since radial migration to the cortex occurs by the extension of a leading neurite-like process (Rakic, 1972), there may be many analogies and conserved signaling pathways involved in both neuronal migration and axon outgrowth.

The similarity of the *scm* phenotype to *reeler* (Gonzalez et al., unpublished data) suggests that the two genes are part of a single genetic pathway. The *reeler* mutation is not cell autonomous (Mikoshiba et al., 1985), consistent with the result that Reelin is a secreted protein (D'Arcangelo et al., 1997). The observation that Reelin is synthesized and localized normally in *scm* mice (Goldowitz et al., 1997; Gonzalez et al., unpublished data) suggested that *scm* may encode part of the receptor signaling system for Reelin, given the precedents for ligand-receptor mutations often giving similar phenotypes (e.g., Steel/c-kit and Notch/Delta). The probable identification of *scm* as *mdab1*, encoding a protein evidently involved in signal transduction at the plasma membrane, is consistent with the view that the *scm* mutation is involved in receptor signaling, although mDab1 is unlikely to represent the receptor protein itself. Hence, the receptor protein for Reelin remains unidentified, although cloning of proteins that bind mDab1 may help define it. mDab1 has additional vertebrate homologs including p96/mDab2 (Xu et al., 1995) and DOC2 (Albertsen et al., 1996). p96 is activated in response to growth factor signaling (Xu et al., 1995), raising the possibility that neural growth factor receptors may also lie upstream of mDab1.

Several other genes cause phenotypes with some similarities to *reeler* and *scm*, including mice mutant for *cdk5* (Ohshima et al., 1996) and for *p35* (Chae et al., 1997), whose protein product binds to and regulates Cdk5. In mice, Cdk5 seems to have no role in cell cycle control and instead is expressed in postmitotic neurons and appears necessary for their normal migration and development. The *cdk5* mutant differs from *reeler* and *scm* in suffering neonatal lethality, but resembles *reeler* and *scm* in having a disruption of normal cortical layering, and associated cerebellar hypoplasia (Ohshima et al., 1996). The *cdk5* mutant phenotype has not been studied to determine whether it shows the same dispersed but roughly inverted pattern of neuronal birth dates that characterizes *reeler* (Caviness, 1982) mice and *scm* mice (Gonzalez et al., unpublished data). Moreover, *p35* mice are less severely affected in cerebellar and hippocampal development than are *reeler* and *scm*, and the inversion of cortical layering in *p35* mutants appears more precise (Chae et al., 1997). Therefore, the genetic relationships between *reeler*, *scm*, *cdk5*, and *p35* are not yet clear. However, the rapidly increasing number of genetically and molecularly characterized mutants that affect the layering of the cortex promises to allow an unprecedented dissection of the mechanisms of neuronal migration.

Experimental Procedures

Genetic Crosses

Mice were cared for according to animal protocols approved by the IACUCs of the Beth Israel Deaconess Medical Center and Harvard Medical School. Mice were housed according to standard methods. The scm cross was begun by outcrossing scm/scm females from a mixed Dc/LE and C3HeB/FeJ background with $^{+/+}$ C57BL/6 males purchased from the Jackson Laboratory (Bar Harbor, ME). Subsequent progeny were intercrossed. Offspring were typed at the scm locus by 1) observation of abnormal gait, 2) brain morphology, and/ or 3) further breeding (in the case of animals with normal phenotype). Animals of known scm genotype were then analyzed for polymorphic microsatellite markers. The C57BL/KsJ-m$^{+/+}$db × MA/MyJ cross was described previously (Chua et al., 1996).

Microsatellite Markers

DNA isolation and microsatellite marker analysis used standard techniques reported elsewhere (Chua et al., 1996).

Library Screening

The MIT/Whitehead YAC library was purchased as pooled samples suitable for analysis using PCR (Research Genetics, Huntsville, AL). PCR screening was carried out according to the manufacturer's directions. One screen of the Whitehead YAC library was performed commercially by Research Genetics. One screen of a BAC library prepared from the 129 mouse strain was performed commercially by Research Genetics, using a PCR-generated probe covering nt 177–626 of the cDNA sequence of mdab1.

YAC DNA Sequencing

IRS–PCR was performed using DNA prepared from yeast carrying the three YACs containing D4Mit29. IRS–PCR was performed using primer B1MvsCh (Hunter et al., 1994) and the following conditions: 5 min at 94°C followed by 40 cycles of 10 s at 94°; 30 s at 50°; 2 min at 72°; followed by a final 10 min at 72°. PCR products were pooled and cloned into a "TA" cloning vector (Invitrogen). Colonies were screened for inserts using blue-white selection on IPTG/Xgal plates. Bacteria from each white colony were lysed by heating at 95°C for 10 min in PCR buffer with 0.5% Tween-20. The resulting crude DNA extract was used for PCR with vector primers without further purification to determine the size of inserts. Clones with inserts of different size were sequenced using universal F and R primers on an ABI 377 automated DNA sequencer. Sequences were analyzed using BLAST NR, BLAST EST, TIGR, and GRAIL2.

Northern and Southern Blotting

A standard mouse embryo multiple tissue Northern blot was purchased from Clontech (Palo Alto, CA) and contained mouse embryo polyA-selected RNA from embryonic day 7 (E7), E11, E15, and E17 age animals. Carefully marked size standards allowed accurate determination of transcript sizes. Additional Northern blots were prepared either from total RNA (4–30 μg/lane) or using polyA-selected RNA prepared from wt, scm/scm, or scm/+ mice ages P0–adult. polyA-selection of RNA was performed using the Oligotex direct mRNA kit (Qiagen, Santa Clara, CA) according to the manufacturer's instructions, starting with 200 μg of total RNA isolated from adult or juvenile mice of known scm genotype. The entire product of polyA-selection of 200 μg of total RNA (~2% yield, corresponding to 2–4 μg of polyA-selected RNA) was loaded in each lane. Running and transfer of Northern blots were performed using Nylon membranes and standard techniques (Ausubel et al., 1994). The probe for the common 5′ end consisted of the PCR product of primers C and E (Table 1); the probe for the 3′ end of 555/271 consisted of the product of primers L and O. Blots were hybridized with ^{32}P-labeled probes using ExpressHyb Hybridization solution (Clontech) according to the manufacturer's directions, washed at moderate stringency, and exposed to autoradiographic film at −70°C with intensifying screens.

Southern blots were prepared by digesting genomic DNA from mice of known scm genotype, beginning with 10 μg of DNA per lane. Digests were performed according to conditions recommended by the manufacturer. Digests were separated on 0.8% agarose gels and transferred to Nylon membranes according to standard techniques (Ausubel et al., 1994). DNA was cross-linked to the membranes using ultraviolet irradiation. Blots were hybridized using ^{32}P-labeled probes using ExpressHyb solution, washed at high stringency, and exposed to autoradiographic film at −70°C with intensifying screens.

RT–PCR

Total RNA (1 μg/reaction) from mouse brain of known scm genotype was reverse-transcribed to make cDNA using Superscript RT (GIBCO/Life Technologies, Gaithersburg, MD), according to the manufacturer's instructions. PCR primers complementary to mdab1 were picked using the Primer 3 program (Whitehead Institute/MIT Center for Genome Research, 1996). PCR reactions began with 1–2 μl of a 20 μl RT-reaction, and used Promega Taq polymerase and the manufacturer's supplied buffers and instructions. Long PCR reactions were performed using the ELONGASE Enzyme Mix (Life Technologies), or the Advantage Klentaq polymerase mix (Clontech, Palo Alto, CA) according to the manufacturer's instructions. PCR products were separated on agarose gels.

DNA Sequence Analysis

DNA sequencing was performed using standard techniques on an ABI 377 automated sequencer, and DNA sequences were constructed, edited, and analyzed using the Sequencher program. All DNA sequences were analyzed using the BLAST program to detect matches to previously known DNA sequence.

Vectorette PCR

Vectorette PCR of genomic sequences adjoining known sequences was performed as previously described for isolation of YAC ends (Ogilvie and James, 1996) with minor modifications. Genomic DNA from scm/scm homozygotes, normal DC/Le mice (purchased from Jackson Laboratory), and normal C3H × C57BL/6 hybrid mice (1 μg each), or DNA from BACs (100 ng) was digested with resriction enzymes (RsaI, EcoRV, AluI, and PvuII) for 1.5 hr in 30 μl reactions. Enzymes were inactivated by heat (65°C for 20 min for PvuII and EcoRV) or protease (Qiagen protease, 1 μl, at 50°C for 30 min, followed by heat inactivation of the protease at 75°C for 30 min). Vectorette primers were identical to those published (Ogilvie and James, 1996) and were preannealed by heating equal quantities of top and bottom vector (Ogilvie and James, 1996) (1 pM/μl) from 85°C–25°C over 40 min. Annealed vectorette primer (2 μl) was added to digested DNA along with 4 μl of ATP (10 mM), 2 μl of dH$_2$O, and 2 μl (2 Weiss U) of T4 DNA ligase (Boehringer Mannheim), and incubated at room temperature for 1 hr. Ligase was inactivated at 65°C for 20 min, and prepared DNA was diluted 10-fold (BAC DNA) or 2-fold (genomic DNA), with 1 μl of the final solution used as a PCR template using gene-specific primers (Table 1) and the vectorette primer. PCR was performed using Klentaq (Clontech) according to the manufacturer's directions and recommended annealing temperatures. Some vectorette PCR products were amplified a second time (after 200-fold dilution) using nested gene-specific and nested vectorette primers (Ogilvie and James, 1996). PCR products were isolated from agarose gels using Geneclean 2 (Bio101, Vista, CA) and sequenced.

References

Albertsen, H.M., Smith, S.A., Melis, R., Williams, B., Holik, P., Stevens, J., and White, R. (1996). Sequence, genomic structure, and chromosomal assignment of human DOC-2. Genomics 33, 207–213.

Amariglio, N., and Rechavi, G. (1993). Insertional mutagenesis by transposable elements in the mammalian genome. Environ. Mol. Mutagen. 21, 212–218.

Ausubel, F., Brent, R., Kingston, R.E., Moore, D.D., Seidman, J.G., Smith, J.A., and Struhl, K., eds. (1994). Current Protocols in Molecular Biology. (New York: Wiley).

Bar, I., Lambert de Rouvroit, C., Royaux, I., Krizman, D.B., Dernoncourt, C., Ruelle, D., Beckers, M.C., and Goffinet, A.M. (1995). A YAC contig containing the reeler locus with preliminary characterization of candidate gene fragments. Genomics 26, 543–549.

Beckers, M.-C., Bar, I., Huynh-Thu, T., Dernoncourt, C., Brunialti, A.L., Montagutelli, X., Guenet, J.-L., and Goffinet, A.M. (1994). A high resolution genetic map of mouse chromosome 5 encompassing the reeler (rl) locus. Genomics 23, 685–690.

Beggs, H.E., Soriano, P., and Maness, P.F. (1994). NCAM-dependent neurite outgrowth is inhibited in neurons from Fyn-minus mice. J. Cell Biol. 127, 825–833.

Beggs, H.E., Baragona, S.C., Hemperly, J.J., and Maness, P.F. (1997). NCAM140 interacts with the focal adhesion kinase p125(fak) and the SRC-related tyrosine kinase p59(fyn). J. Biol. Chem. 272, 8310–8319.

Caviness, V.S., Jr. (1982). Neocortical histogenesis and reeler mice: A developmental study based upon [3H]thymidine autoradiography. Dev. Brain Res. 4, 293–302.

Chae, T., Kwo, Y.T., Bronson, R., Dikkes, P., Li, E., and Tsai, L.H. (1997). Mice lacking p35, a neuronal specific activator of Cdk5, display cortical lamination defects, seizures, and adult lethality. Neuron 18, 29–42.

Chua, S.C., Jr., Chung, W.K., Wu-Peng, S., Zhang, Y., Liu, S.-M., Tartaglia, L., and Leibel, R.L. (1996). Phenotypes of mouse diabetes and rat fatty acid due to mutations in the OB (Leptin) receptor. Science 271, 994–996.

Copeland, N.G., Gilbert, D.J., Jenkins, N.A., Nadeau, J.H., Eppig, J.T., Maltais, L.J., Miller, J.C., Dietrich, W.F., Steen, R.G., et al. (1993). Genome maps IV. Science 262, 67.

Cox, M.E., and Maness, P.F. (1992). Protein tyrosine kinases in nervous system development. Semin. Cell Biol. 3, 117–126.

D'Arcangelo, G., Miao, G.G., Chen, S.C., Soares, H.D., Morgan, J.I., and Curran, T. (1995). A protein related to extracellular matrix proteins deleted in the mouse mutant reeler. Nature 374, 719–723.

D'Arcangelo, G., Nakajima, K., Miyata, T., Ogawa, M., Mikoshiba, K., and Curran, T. (1997). Reelin is a secreted glycoprotein recognized by the CR-50 monoclonal antibody. J. Neurosci. 17, 23–41.

Dietrich, W.F., Miller, J.C., Steen, R.G., Merchant, M., Damron, D., Nahf, R., Gross, A., Joyce, D.C., Wessel, M., et al. (1994). A genetic map of the mouse with 4,006 simple sequence length polymorphisms. Nature Genet. 7, 220–245.

Dietrich, W.F., Miller, J., Steen, R., Merchant, M.A., Damron-Boles, D., Husain, Z., Dredge, R., Daly, M.J., Ingalls, K.A., et al. (1996). A comprehensive genetic map of the mouse genome. Nature 380, 149–152.

Duhl, D.M., Vrieling, H., Miller, K.A., Wolff, G.L., and Barsh, G.S. (1994). Neomorphic agouti mutations in obese yellow mice. Nature Genet. 8, 59–65.

Falconer, D. (1951). Two new mutants, 'trembler' and 'reeler,' with neurological actions in the house mouse (Mus Musculus). J. Genet. 50, 192–201.

Gertler, F.B., Hill, K.K., Clark, M.J., and Hoffmann, F.M. (1993). Dosage-sensitive modifiers of Drosophila abl tyrosine kinase function: prospero, a regulator of axonal outgrowth, and disabled, a novel tyrosine kinase substrate. Genes Dev. 7, 441–453.

Gertler, F.B., Niebuhr, K., Reinhard, M., Wehland, J., and Soriano, P. (1996). Mena, a relative of VASP and Drosophila Enabled, is implicated in the control of microfilament dynamics. Cell 87, 227–239.

Goffinet, A.M. (1984). Events governing organization of postmigratory neurons: studies on brain development in normal and reeler mice. Brain Res. Rev. 7, 261–296.

Goffinet, A.M. (1992). The reeler gene: a clue to brain development and evolution. Int. J. Dev. Biol. 36, 101–107.

Goldowitz, D., Cushing, R.C., Laywell, E., D'Arcangelo, G., Sheldon, M., Sweet, H., Davisson, M., Steindler, D., and Curran, T. (1997). Cerebellar disorganization characteristic of reeler in scrambler mutant mice despite presence of Reelin. J. Neurosci., in press.

Grant, S.G., O'Dell, T.J., Karl, K.A., Stein, P.L., Soriano, P. and Kandel, E.R. (1992). Impaired long-term potentiation, spatial learning, and hippocampal development in fyn mutant mice. Science 258, 1903–1910.

Hamilton, B.A., Smith, D.J., Mueller, K.L., Kerrebrock, A.W., Bronson, R.T., van Berkel, V., Daly, M.J., Kruglyak, L., Reeve, M.P., et al. (1997). The vibrator mutation causes neurodegeneration via reduced expression of PITPα: positional complementation cloning and extragenic suppression. Neuron 18, 711–722.

Hirotsune, S., Takahara, T., Sasaki, N., Hirose, K., Yoshiki, A., Ohashi, T., Kusakabe, M., Murakami, Y., Muramatsu, M., et al. (1995). The reeler gene encodes a protein with an EGF-like motif expressed by pioneer neurons. Nature Genet. 10, 77–83.

Howell, B.W., Gertler, F.B., and Cooper, J.A. (1997). Mouse disabled (mDab1): a Src binding protein implicated in neuronal development. EMBO J. 16, 121–132.

Hunter, K., Ontiveros, S., Watson, M., Stanton, V., Jr., Gutierrez, P., Bhat, D., Rochelle, J., Graw, S., Ton, C., et al. (1994). Rapid and efficient construction of yeast artificial chromosome contigs in the mouse genome with interspersed repetitive sequence PCR (IRS–PCR): generation of a 5-cM, >5 megabase contig on mouse chromosome 1. Mammalian Genome 5, 597–607.

Hunter, K., Riba, L., Schalkwyk, L., Clark, M., Resenchuk, S., Beeghly, A., Su, J., Tinkov, F., Lee, P., et al. (1996). Toward the construction of integrated physical and genetic maps of the mouse genome using interspersed repetitive sequence PCR (IRS–PCR) genomics. Genome Res. 6, 290–299.

Ignelzi, M.A., Jr., Miller, D.R., Soriano, P., and Maness, P.F. (1994). Impaired neurite outgrowth of src-minus cerebellar neurons on the cell adhesion molecule L1. Neuron 12, 873–884.

Imamoto, A., and Soriano, P. (1993). Disruption of the csk gene, encoding a negative regulator of Src family tyrosine kinases, leads to neural tube defects and embryonic lethality in mice. Cell 73, 1117–1124.

Kuff, E.L., and Lueders, K.K. (1988). The intracisternal A-particle gene family: structure and functional aspects. Adv. Cancer Res. 51, 183–276.

Lueders, K.K., and Kuff, E.L. (1987). Intracisternal A-particle genes: identification in the genome of Mus musculus and comparison of multiple isolates from a mouse gene library. Proc. Natl. Acad. Sci. USA 77, 3571–3575.

Michaud, E.J., van Vugt, M.J., Bultman, S.J., Sweet, H.O., Davisson, M.T., and Woychik, R.P. (1994). Differential expression of a new dominant agouti allele (A^iapy) is correlated with methylation status and is influenced by parental lineage. Genes Dev. 8, 1463–1472.

Mikoshiba, K., Yokoyama, M., Nishimura, Y., Katsuki, M., Nomura, T., and Tsukada, Y. (1985). Mosaic expression of the Reeler and normal phenotypes in the cerebral cortex in Reeler-normal chimeras at a late embryonic stage. Dev. Growth Differ. 27, 737–744.

Ogilvie, D.J., and James, L.A. (1996). End rescue from YAC's using the vectorette. Methods in Molecular Biology (Totowa, NJ: Humana Press, Inc.), pp. 131–144.

Ohshima, T., Ward, J.M., Huh, C.G., Longenecker, G., Veeranna, A., Pant, H.C., Brady, R.O., Martin, L.J., and Kulkarni, A.B. (1996). Targeted disruption of the cyclin-dependent kinase 5 gene results in abnormal corticogenesis, neuronal pathology and perinatal death. Proc. Natl. Acad. Sci. USA 93, 11173–11178.

Rakic, P. (1972). Mode of cell migration to the superficial layers of fetal monkey neocortex. J. Comp. Neurol. 145, 61–84.

Royaux, I., Bernier, B., Montgomery, J.C., Flaherty, L., and Goffinet, A.M. (1997). Reln^rlAlb2, an allele of Reeler isolated from a chlorambucil

screen, is due to an IAP insertion with exon skipping. Genomics *42*, 479–482.

Rusanescu, G., Qi, H., Thomas, S.M., Brugge, J.S., and Halegoua, S. (1995). Calcium influx induces neurite growth through a Src–Ras signaling cassette. Neuron *15*, 1415–1425.

Schwartzberg, P., Stall, A., Hardin, J., Bowdish, K., Humaran, T., Boast, S., Harbison, M., Robertson, E., and Goff, S. (1991). Mice homozygous for the ablm1 mutation show poor viability and depletion of selected B and T cell populations. Cell *65*, 1165–1175.

Shapiro, M.B., and Senapathy, P. (1987). RNA splice junctions of different classes of eukaryotes: sequence statistics and functional implications in gene expression. Nucleic Acids Res. *15*, 7155–7174.

Stein, P., Lee, H., Rich, S., and Soriano, P. (1992). pp59fyn mutant mice display differential signaling in thymocytes and peripheral T cells. Cell *70*, 741–750.

Stein, P., Vogel, H., and Soriano, P. (1994). Combined deficiencies of Src, Fyn, and Yes tyrosine kinases in mutant mice. Genes Dev. *8*, 1999–2007.

Sweet, H.O., Bronson, R., Johnson, K., Cook, S., and Davisson, M.T. (1996). Scrambler, a new neurological mutation of the mouse with abnormalities of neuronal migration. Mammalian Genome *7*, 798–802.

The Mouse Genome Database (1997). (Bar Harbor, ME: Mouse Genome Informatics and Laboratory, The Jackson Laboratory).

Thomas, S.M., Soriano, P., and Imamoto, A. (1995). Specific and redundant roles of Src and Fyn in organizing the cytoskeleton. Nature *376*, 267–271.

Tybulewicz, V.L., Crawford, C.E., Jackson, P.K., Bronson, R.T., and Mulligan, R.C. (1991). Neonatal lethality and lymphopenia in mice with a homozygous disruption of the c-abl proto-oncogene. Cell *65*, 1153–1163.

Whitehead Institute/MIT Center for Genome Research. (1996). Genomic map of the mouse, database release 10. (Cambridge, MA: MIT Press).

Xu, X.X., Yang, W., Jackowski, S., and Rock, C.O. (1995). Cloning of a novel phosphoprotein regulated by colony-stimulating factor 1 shares a domain with the Drosophila disabled gene product. J. Biol. Chem. *270*, 14184–14191.

Note Added in Proof

The work referred to as González et al., unpublished data is a completed body of work presently under review: González, J. Russo, C. J., Goldowitz, D., Sweet, H. D., Davisson, M. T., and Walsh, C. A. Birthdate and cell marker analysis of scrambler: a novel mutation affecting cortical development with a reeler-like phenotype.